Bio-precipitation of arsenic and antimony in a sulfate-reducing bioreactor treating real acid mine drainage water

Elia Laroche, Catherine Joulian, Cédric Duée, Corinne Casiot, Marina Héry, Fabienne Battaglia-Brunet

OXFORD UNIVERSITY PRESS | FEMS Microbiology Ecology

http://mc.manuscriptcentral.com/fems

Bio-precipitation of antimony in a sulfate-reducing bioreactor treating a real As-rich acid mine drainage water

Journal:	*FEMS Microbiology Ecology*
Manuscript ID	Draft
Manuscript Type:	Research article
Date Submitted by the Author:	n/a
Complete List of Authors:	Laroche, Elia; Bureau de Recherches Geologiques et Minieres, Water, Environment, Process Development and Analysis Division; HydroSciences Montpellier, Montpellier CNRS, IRD Joulian, Catherine; Bureau de Recherches Geologiques et Minieres, Water, Environment, Process Development and Analysis Division Duee, Cédric; BRGM, Water, Environment, Process Development and Analysis Division Casiot-Marouani, Corinne; HydroSciences Montpellier, University of Montpellier, CNRS, IRD, Montpellier, France hery, marina; HydroSciences Montpellier, University of Montpellier, CNRS, IRD, Montpellier, France Battaglia-Brunet, Fabienne ; BRGM, Water, Environment, Process Development and Analysis Division; ISTO, Université d'Orléans, CNRS, BRGM
Keywords:	antimony, arsenic, bioremediation, acid mine drainage, sulfate-reducing bacteria, Desulfosporosinus

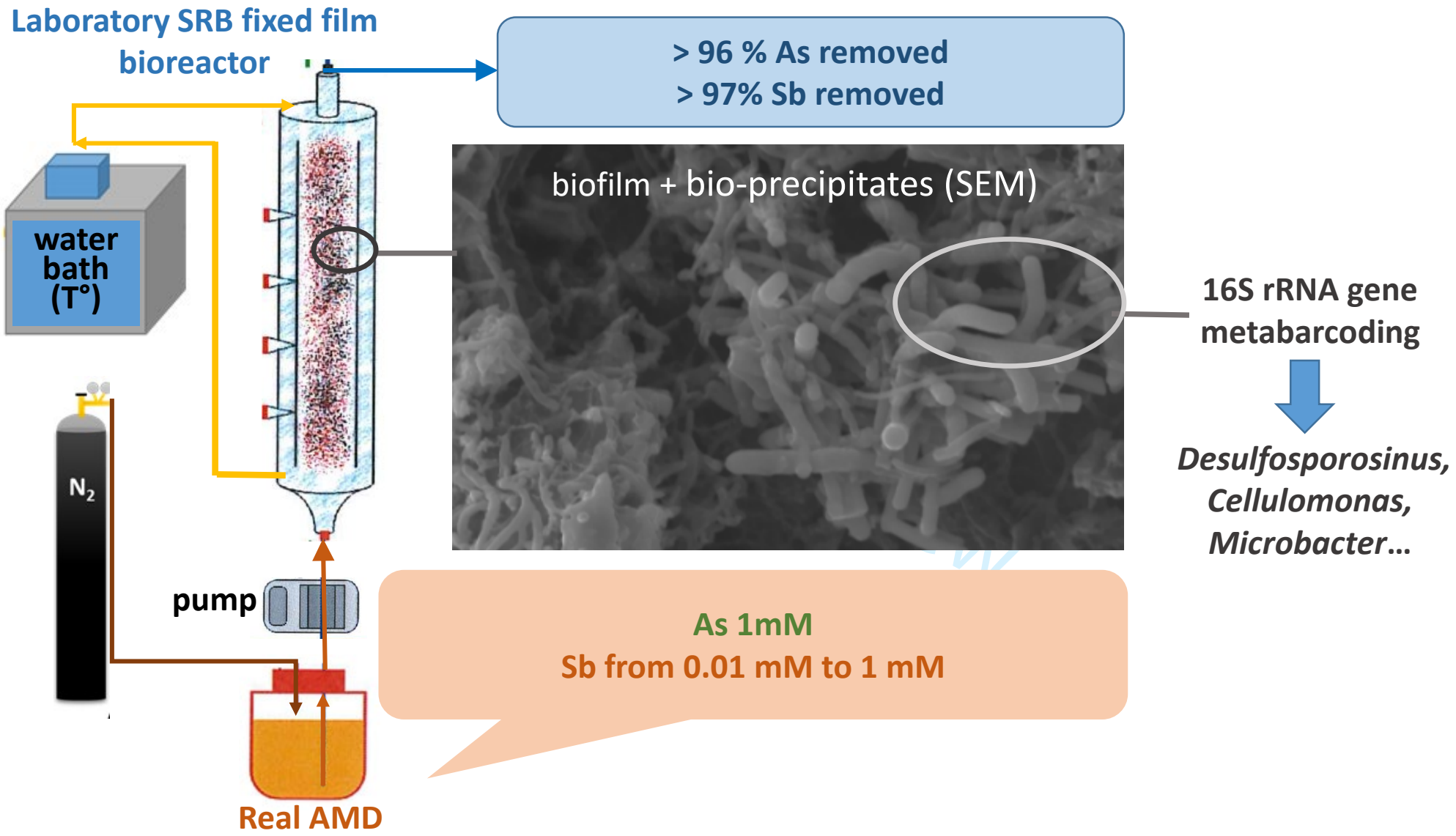
Laboratory SRB fixed film bioreactor
> 96 % As removed
> 97% Sb removed
water bath (T°)
biofilm + bio-precipitates (SEM)
16S rRNA gene metabarcoding
Desulfosporosinus, Cellulomonas, Microbacter…
N2
pump
As 1mM
Sb from 0.01 mM to 1 mM
Real AMD

Bio-precipitation of antimony in a sulfate-reducing bioreactor treating a real As-rich acid mine drainage water

Elia Laroche[1,2], Catherine Joulian[1], Cédric Duee[1], Corinne Casiot[2], Marina Héry[2], Fabienne Battaglia-Brunet[1,3,*]

[1]BRGM, F-45060 Orléans, France

[2]HydroSciences Montpellier, Univ Montpellier, CNRS, IRD, Montpellier, France

[3]ISTO, UMR7327, Université d'Orléans, CNRS, BRGM, F-45071 Orléans, France

*Correspondin author: f.battaglia@brgm.fr

Abstract:

Arsenic (As) and antimony (Sb) can be disseminated from mining sites to aquatic ecosystems by acid mine drainage (AMD). Here, the possibility to remove As and Sb concomitantly from acidic waters by precipitation of sulphides induced by sulfate-reducing bacteria (SRB) was investigated in a fixed-bed column bioreactor. The real AMD water used to feed the bioreactor contained nearly 1 mM As and increasing Sb concentrations (0.008 ± 0.006 to 1.01 ± 0.07 mM) in order to reach a molar ratio Sb/As = 1. Results showed that the addition of Sb did not affect the efficiency of As bio-precipitation. Sb was removed efficiently (up to 97.9% removal) between the inlet and outlet of the bioreactor, together with As (up to 99.3% removal) in all conditions. Sb was generally removed as it entered the bioreactor. Appreciable sulfate reduction occurred in the bioreactor and could be linked to the stable presence of a

major SRB OTU affiliated to the *Desulfosporinus* genus. The bacterial community included polymer degraders, fermenters, and acetate degraders. Results suggested that sulfate-reduction could be a suitable bioremediation process for the simultaneous removal of Sb and As from AMD.

Keywords: antimony, arsenic, bioremediation, acid mine drainage, sulfate-reducing bacteria, *Desulfosporosinus*

Introduction

Elevated concentrations of arsenic (As) and antimony (Sb) have been measured in diverse natural environments due to anthropogenic emissions (Smedley and Kinniburgh, 2002; Herath et al., 2017). These toxic metalloids are considered by the European Union and United States Environmental Protection Agency as pollutants of priority interest (Council of the European Communities, 1976; US EPA, 1982). Mining activities are a major source of As and Sb dissemination in the environment (Smedley and Kinniburgh, 2002; He et al., 2019). Wastes generated by mineral extraction can contain up to 10,000 ppm As and 1,000 ppm Sb associated with sulfide minerals (Smedley and Kinniburgh, 2002; Wu et al., 2011; Cidu et al., 2014). As result of inappropriate waste storage, oxidation of the sulfide minerals can generate mine drainage characterised by high concentrations of these elements, which can enter aquatic ecosystems (Manaka et al., 2007; Resongles et al., 2013; Paikaray, 2015; Sun et al., 2016). However, solubilised As and Sb can be immobilised by co-precipitation with insoluble metal (hydro)oxides (Cullen and Reimer, 1989; Filella et al., 2002). These processes have been exploited in water treatment technology, and the combined removal of these two elements following iron (Fe) addition was considered. However, variable efficiencies of As and Sb adsorption onto iron compounds have been reported due to synergic or competitive behaviour

according to the speciation of these elements (Lan et al., 2016; Qi and Pichler, 2017; Inam et al., 2018; Wu et al., 2018) and pH (Inam et al., 2018). Moreover, the disadvantages of Fe-based treatments are the need of a constant maintenance and elevated costs. The development of passive treatment systems exploiting biological processes is a promising low-cost strategy for the remediation of metals and metalloids present in acid mine drainages (Skousen et al., 2000). Biological processes including direct bio-reduction or bio-oxidation can be exploited in bioremediation solutions. Therefore, Kujala et al. (2022) studied the passive treatment of mining-affected neutral water containing both Sb and As (around 2 and 0.5 µM respectively) in peatlands, involving bio-oxidation and bio-reduction processes. Among the anaerobic biological reactions, microbial sulfate-reduction has proven itself as an efficient way to remove metals from mine waters at large scale (Mattes et al., 2011). In anaerobic bioreactors or wetlands, the biological sulfide precipitation exclusively precipitates elements that are already in the mine water. No external element (calcium or iron) is added, thus the final mass of produced waste is lower than in competitor acid mine drainage technologies (Battaglia-Brunet et al., 2021). Sulfate reduction has been shown to efficiently treat As and Sb individually (Wang et al., 2013; Zhang et al., 2016; Alam and McPhedran, 2019; Xi et al., 2020, Chen et al., 2020). Liu et al. (2018) also reported the concomitant removal of 5 mg/L As and Sb from artificial waste water at neutral pH by bacterial sulfate reduction. In this batch experiment, the removal of As depended on the presence of Fe(II) in the synthetic medium, whereas Sb was removed even in absence of Fe. Although microbial sulfate-reduction has been described for a long time as a bioprocess inhibited in acidic conditions, progress has been made recently in the field of bio-precipitation of sulfides at low pH (Ňancucheo and Johnson, 2012 and 2014). More specifically, bio-precipitation of arsenic sulfide at low pH was reported (Battaglia-Brunet et al., 2012; Le Pape et al., 2017). From a chemical point of view, precipitation of As sulfide should be favored at low pH, while soluble thio-As

complexes form at neutral and alkaline pH. The same geochemical behaviour was observed with Sb in geothermal systems (Planer-Friedrich and Scheinost, 2011). The pH is likely to affect the biogeochemical behaviour of Sb in sulfate-reducing bioreactors, as it was the case for As. Finally, the combined removal by bacterial sulfate-reduction of both As and Sb, when they co-occur in an AMD has not yet been studied. In this context, the aim of the present study was to evaluate the efficiency of an upflow anaerobic fixed-bed column reactor to treat concomitantly As and Sb present in an AMD by biological sulfate-reduction in acidic conditions. The removal of these pollutants was investigated during ten months along the bioreactor in which Sb concentration was increased progressively. Physico-chemical parameters were monitored, together with mineral characterisation of the bioprecipitates. The spatial and temporal evolution of the bacterial community colonizing the reactor was investigated by 16S rRNA gene metabarcoding. Both results will document the understanding of the biogeochemical behaviour of As and Sb, in the context of sulfate reduction under acidic conditions.

Material and methods

Bioreactor design and operating conditions

The lab-scale experiment was performed in a fixed-bed reactor, consisting of a 360 mm glass column with an internal diameter of 36 mm (Fig. 1). A water jacket regulated the column temperature at 25°C during the experiment and rubber-stopped sampling ports allowed liquid sampling from the middle, bottom and upper levels. The column was sterilised by autoclaving (120°C, 30 min) before filling with sterile materials composed of a mixture of pozzolana and nutritive agar in order to enhance both bacterial attachment and growth, as previously described (Battaglia-Brunet et al., 2021). The filling mixture was prepared with a total volume

of 400 mL pozzolana, 400 mL agar at 25 g/L, 20 mL nutritive solution at pH 4.5 (20 g/L yeast extract and 7.8 g/L KH_2PO_4) and 0.4 mL trace element solution (3 g/L EDTA; 1.1 g/L $FeSO_4$, $7H_2O$; 65 mg/L $MnSO_4$, H_2O; 89 mg/L $ZnSO_4$, $7H_2O$; 28 mg/L $NiSO_4$, $7H_2O$; 18 mg/L Na_2MoO_4, $2H_2O$; 0.3 g/L H_3BO_3; 2 mg/L $CuCl_2$; 130 mg/L $CoSO_4$, $7H_2O$).

The filled column was de-oxygenated by flushing with sterile N_2 during three days, then inoculated with an acid tolerant microbial consortium containing sulfate-reducing bacteria (SRB) originating from the AMD of Carnoulès, France (Le Pape et al., 2017). Ten mL of this inoculum were centrifuged and the pellet stored at -80°C prior molecular analyses. A first step promoting bacterial growth inside the column was performed in batch mode during 23 days. Then, the column was fed in continuous mode with AMD water sampled in January 2016 at the Carnoulès mine (Gard, France) and stored at 4°C under nitrogen until use. The main characteristics of this AMD are a pH close to 3, around 100 mg/L total dissolved As, 1000 mg/L total dissolved Fe, 20 mg/L total dissolved Zn (Le Pape et al., 2017), and less than 1 mg/L total dissolved Sb (Resongles et al., 2013). For the experiment, its pH was increased between pH 4.0 and 4.5 by adding NaOH. The water was filtered (0.22 µm) and complemented with 0.5 g/L glycerol as electron donor for the SRB. The feeding water was maintained in anaerobic condition under N_2 atmosphere.

The variable parameter was the Sb concentration in the feed water: it was increased by adding Sb in the real AMD water, as potassium Sb(III) tartrate, in three steps (corresponding to phase 1, 2 and 3) up to the molar equivalence between Sb and the As naturally present in the AMD. The experimental parameters of each phase, flow rate, pH, As and Sb concentration in the feed solution prepared with the real AMD, are summarised in Table 1. Analyses of exploitable data started after the physico-chemical parameters (outlet pH, As, and Fe concentration in the outlet) had stabilised for each Sb concentration in the feed in order to compare the acquired results during each experimental condition.

Monitoring

Inlet and outlet waters were collected under anaerobic conditions and monitored over a 217 days period after the first 59 days dedicated to stabilisation of physico-chemical parameters. The real flow-rate was calculated by weighing the cumulated outlet water collected in a bottle (every day except Saturdays and Sundays). Inlet and outlet water pH were measured, and 10 mL were filtered at 0.45 µm, acidified with one drop of concentrated nitric acid and stored at 4°C until chemical analyses. The outlet water was sampled every day whereas the inlet water sampling was done at each renewal of feed water.

Vertical profiles of physico-chemical and microbial parameters were determined at the end of each phase from liquid samples taken along the column. Five mL of liquid samples were collected in triplicate inside the column through the bottom, middle and upper septa with a sterile syringe. These samples were mainly constituted of solution, with bacteria in suspension, but could also contain precipitates (with or without attached bacteria). Triplicate samples were also collected from inlet and outlet water bottles. Samples were filtered with a sterile 0.22 µm cellulose acetate filter which was stored at -80°C for molecular analyses. The filtrate was acidified and kept at 4°C for chemical analysis.

At the end of the experiment (day 217), the column was opened in a glovebox under N_2 atmosphere to collect bioprecipitates deposited on the solid filling materials. Triplicate samples of solids were taken from the bottom, middle and upper parts of the column and stored at -80°C until molecular analysis. Solid samples were also collected along the column and dried under N_2 flux in anaerobic Hungate glass tubes for mineralogical characterisation.

Chemical analyses

Total As and Fe concentrations were monitored on outlet samples to check that stabilisation was reached before changing the operating conditions, by Atomic Absorption

Spectrophotometry (AAS, Varian SpectrAA 220 FS). After stabilisation, a more complete chemical characterisation was performed on selected water samples from outlet and inlet (three for each feed phase, except the Sb concentration from the inlet water in phase 1 in duplicate, Table 1) and from the vertical profiles collected at the end of each phase. In these samples, total dissolved concentrations of As, Sb, Fe, S and other elements (Zn, Tl, Pb) were analysed using ICP-MS on the AETE-ISO platform (University of Montpellier).

Characterisation of the bioprecipitates

The bioprecipitates collected at the end of the experiment were characterised by scanning electron microscopy (SEM). Prior to SEM, samples were submitted to plasma cleaner (Gambetti, Colibri, 300 s under Ar plasma) in order to remove organic phases. Samples were then covered with a 20 nm carbon coating (Cressington, Carbon Coater 208C) to make them conductive. The SEM images were acquired on a field emission gun scanning electron microscope MIRA 3 XMU (TESCAN, Brno, Czech Republic), under high vacuum conditions with a 15 kV beam. EDS spectra and element mappings were recorded using an EDAX Pegasus EDS system.

Molecular analyses

Genomic DNA was extracted from the pellet of the inoculum, frozen filters (5 mL aliquot) and bioprecipitates (between 0.5 and 0.8 g), using the FastDNA Spin Kit for soil according to the manufacturer's recommendations (MP Biomedicals, Illkirch, France), with the FastPrep®-24 instrument at a speed of 5 ms^{-1} for 30s. DNA extracts were quantified with the Quantifluor dsDNA sample kit and the Quantus fluorometer, according to the manufacturer's instructions (Promega, Madison, WI, USA), and stored at -20°C.

Bacterial diversity was determined by 16S rRNA gene metabarcoding. Libraries of amplicons and sequencing were performed by MetaHealth metagenomic-based services (CIRAD, PHIM,

Eco&Sols, Montpellier, France). The 16S rRNA V3-V4 gene region was first amplified with primers 341F (5'-CCTACGGGNGGCWGCAG-3') and 785R (5'-GACTACHVGGGTATCTAATCC-3'), in duplicate in a Mastercycler ep 384 (Eppendorf) thermocycler with 20 µL PCR reaction (0.5 g of DNA, 10 µL of Phusion Flash High-Fidelity 2X Master Mix (Thermo Fisher), 300 ng T4 gene 32 (MP Biomedicals), 0.25 µM for forward and reverse primers). The following conditions were applied: initial denaturation at 95°C for 2 min, 25 cycles of 95°C for 30 s, 55°C for 40 s, 72°C for 30 s and a final elongation at 72°C for 10 min. A second PCR was run using primers 341F and 785R modified with Illumina specific overhang sequences to implement dual barcodes. PCR reactions (15 µL) contained: 7.5 µL Biolabs Taq 2X mastermix, 2 µL of 10 µM for forward and reverse primers, and 2 µL of PCR product. The following conditions were applied: initial denaturation at 95°C for 2 min, 8 cycles of 95°C for 30 s, 55°C for 40 s, 72°C for 30 s and a final elongation at 72°C for 10 min. Final amplicons concentrations were quantified on a D5000 ScreenTape bioanalyzer (Agilent) and validated by qPCR on a LC480 real-time thermocycler (Roche), using qPCR primers recommended in Illumina's qPCR protocol and Illumina's PhiX control library as standard (Illumina). All amplicon products and control library (5% PhiX library) were finally sequenced using paired-end Illumina MiSeq sequencing (2×300 bp). The raw datasets are available on the European Nucleotide Archive system under project accession number PRJEB50048.

Bioinformatic analyses

Illumina reads were processed with the bioinformatics pipeline FROGS v 3.2 (Find Rapidly OTUs with Galaxy Solution) (Escudié et al., 2018) available on the GenoToul Galaxy platform (Afgan et al., 2018). Paired-end reads were firstly merged with a maximum of 10% mismatch in the overlapped region with VSERACH. Only sequences with expected length (between 340 and 450 nucleotides), no ambiguous bases (N) were clustered in two steps using

the SWARM algorithm to obtain Operational Taxonomic Units (OTUs) with minimal distance (d g= 1), then with an aggregation distance of 3 (Mahé et al., 2014). The removal of chimeric sequences was performed with VSEARCH with de novo UCHIME method (Edgar et al., 2011; Rognes et al., 2016), combined with a cross-sample validation. A filtering tool was used to select OTU according to their abundance (threshold = 5 $.10^{-5}$, Bokulich et al., 2013), leading to a total of 1,595,159 high quality sequences. Subsampling to the lowest dataset (7,910 reads) was performed by random selection in order to efficiently compare the datasets and avoid biased community comparisons. Each OTU was affiliated against the SILVA reference database (v138). Statistics tools included in FROGS pipeline were used to generate OTU table and to calculate the alpha and beta diversity (diversity indices and bray-Curtis distances).

Statistical analysis

Statistical analyses were performed with R version 3.4.3 (R Core Team, 2018) according to Laroche et al. (2018). The "ade4" R package was used to perform a co-inertia analysis (CIA) and two Principal Component Analyses (PCA) (Dray and Dufour, 2007). These analyses highlighted the common structure between the physico-chemical parameters (pH and dissolved iron, sulfur, arsenic and antimony concentrations) and the dominant bacterial taxa in the liquid samples at each position in the column. These dominant taxa represented more than 90% of the relative abundance of sequences in every sample during the monitoring period. Before the CIA, the physico-chemical and biological variables were respectively standardised and Hellinger transformed (Legendre and Gallagher, 2001). The significance of the analysis was checked with a Monte-Carlo test (999 random permutations).

Results

Evolution of pH

The pH was always increased between the inlet and the outlet water of the bioreactor (Fig. 2A). The average pH increased from 4.29 ± 0.03 to 5.10 ± 0.25 during the phase 1, from 4.03 ± 0.06 to 5.05 ± 0.19 during the phase 2 and from 4.35 ± 0.20 to 4.91 ± 0.29 during phase 3 (Fig. 2B). This pH increase was gradual in phase 1. In phases 2 and 3, there was a strong pH increase (around 1 unit) between the inlet and the bottom of the column, followed by little pH variation (< 0.3 unit) between the bottom and the upper section and finally a pH decreases between the upper section and the outlet.

Removal of As, Sb, Fe and S from the mine water

The reactor removed 96 to 99% of dissolved As, during each of the three phases of experiment (Fig. 3A). Arsenic removal occurred at different levels of the column bioreactor depending on the experimental conditions. At the end of phase 1, 72% of As was removed between the bottom and the middle of the column. In phase 2, As concentration decreased gradually from 0.5 to 0.1 mM from the bottom to the top. In phase 3, As was mainly removed between the feed point and the bottom of the reactor (99.8%).

During phase 1, Sb concentration in the feed solution was that of the natural AMD (less than 0.01 mM), thus it was too low to determine a precise removal rate. Sb removal during the two next phases, in which Sb concentrations were adjusted to about 0.7 and 1 mM, averaged 97% and 98% respectively. Most Sb was removed in the bottom zone of the reactor in each phase (Fig. 3B and C). As for arsenic, its concentration decreased gradually from 0.018 to 0.004 mM along the column in phase 2. The dissolved Sb concentration in the outlet water was always higher than in the upper zone of the bioreactor. This phenomenon, also observed for S and Fe in phase 2, might be explained by oxidation reactions. Despite the constant flow of N_2

flux in the outlet bottle, there may to have been some oxygen diffusion through the outlet pipe. Other toxic chemical substances (Pb, Tl and Zn) present in minor concentrations in the feed water were removed inside the bioreactor (Supplementary Table SM1).

The average dissolved Fe and sulphur (S) concentrations in the inlet water were respectively 21 ± 2 and 38 ± 3 mM (Fig. 3 D and E). Maximum Fe removal reached 20, 35 and 14% in phase 1, 2 and 3, respectively (Fig. 3D). Sulfur removal reached 16, 17, and 11% in phases 1, 2 and 3 respectively. Inside the column, the S concentration decreased gradually from 33.8 to 30.4 mM at the end of the phase 1 (Fig. 3E). For the others phases, it stabilised around 32.3 ± 0.05 mM (phase 2) and 30.0 ± 0.5 mM (phase 3) between bottom and upper section and increased slightly in the outlet water.

Observation of the bioprecipitates

SEM observation of the biofilm-colonised filling materials collected inside the bioreactor revealed the presence of mineral-encrusted rod-shaped bacteria of different sizes, around 5 µm long and 0.5 to 2 µm wide (Fig. 4 A). The EDS spectra of the mineral phases associated with this biofilm revealed major peaks of S and As. However, since the interaction volume of the electron beam is ca. 1 μm^3, it cannot be excluded that part of the EDS signal comes from the surrounding phases. Other zones of the biofilm showed aggregates including rod cells-shaped particles (Fig. 4C), enriched in Sb together with As and S as major peaks on the EDS spectrum (Fig. 4D). The elemental map of one bioprecipitate (Fig. SM2) showed differences between the distribution of As and Sb in the As-Sb-S bearing phase. Moreover, the areas corresponding to high Fe concentrations were distinct to those of high As and Sb concentrations in this bioprecipitate.

Evolution of bacterial diversity

The 16S rRNA genes retrieved by metabarcoding from inoculum, liquid samples and bioprecipitates collected inside the bioreactor were classified into 78 OTUs. Overall, the richness (number of observed OTU) and the Shannon index (reflecting both richness and evenness) indicated a low bacterial diversity in all the samples (Fig. SM3). The highest bacterial diversity was observed in liquids collected at the end of phase 1 in the bottom and in the upper of the column (30 ± 2 OTU observed).

Ten taxa identified at the genus level had relative abundance of reads ≥ 2% in at least one sample (Fig. 5). The inoculum, able to reduce sulfate at acidic pH and enriched from the Carnoulès AMD, was mainly composed of *Desulfosporosinus* (77.0%), *Microbacter* (11.6%) and *Cellulomonas* (10.9%) These three genera were identified in all liquid samples collected inside the column, whatever the level and the phase, with relative sequence abundances varying from 1.9 ± 0.4% to 76.5 ± 5.9% (mean of triplicates) for *Desulfosporosinus*, 4.4 ± 1.3% to 41.3 ± 2.4% for *Cellulomonas* and 16.0 ± 4.6% to 66.5 ± 1.2% for *Microbacter*. Other genera were detected in lower proportions inside the column: *Acidithiobacillus* (0.7 ± 0.2% to 16.9 ± 2.0%), *Luteococcus* (0.3 ± 0.04% to 9.3 ± 1.7%), *Acidocella* (0 to 4.9 ± 1.1%), *Metallibacterium* (0 to 5.1 ± 0.2%), *Sediminibacterium* (0 to 2.6 ± 2.2%), *Streptococcus* (0 to 2.7 ± 4.6%) and *Thiomonas* (0 to 3.1 ± 0.3%). There was a clear evolution in both space and time of the taxonomic composition of bacterial communities inside the column. *Desulfosporosinus* proportions were lower during phases 1 and 2 in all levels (1.9 ± 0.4% to 35.7 ± 8.9%), than in the inoculum. However, it became again dominant (76.5 ± 5.9%) during phase 3 at the bottom of the column. *Cellulomonas* was the dominant genus in bottom and middle column samples in phase 1 (33.9 ± 0.7 and 41.3 ± 2.4%), and co-dominant (41.2 ± 5.8%) in the bottom level in phase 2. *Microbacter* was dominant in the upper level in phase 1 and 2 (53.3 ± 3.9% and 66.5 ± 1.2%) and middle and upper levels in phase 3 (36.6 ± 9.1% and 53.9 ± 10.1). *Luteococcus* was always present but at low relative abundance (less than 9.3

± 1.7%) and particularly during the phases 1 (bottom and middle) and 2 (bottom). *Acidocella* was more abundant in the bottom level during phase 1 (4.9 ± 1.1%); its relative abundance was the lowest during phase 3.

At the end of the experiment (phase 3), the main difference between communities from bioprecipitates and liquid samples was the relative abundance of the *Desulfosporosinus* genus. Its proportion was close for the bottom level and higher for the middle and top levels on the solids (71.6 ± 1.7% bottom, 81.0 ± 1.3% middle and 47.6 ± 5.6% top) than in the liquid (76.5 ± 1.7% bottom, 30.0 ± 15.6% middle and 14.8 ± 2.9% top) samples. It was thus largely dominant in the bioprecipitates collected from bottom and middle levels. *Microbacter*, *Cellulomonas* and *Luteococcus* were also identified in the bioprecipitates.

A co-inertia analysis was performed to interpret the relationship between the physico-chemical parameters and the dominant bacterial taxa (Fig. 6). The Monte-Carlo test revealed a significant co-structure between the physico-chemical and biological variables (p-value = 0.03). Ninety seven percent of the total variance in the two datasets were explained by the first two axes of the CIA. Samples were separated according their position in the column, particularly at the bottom, along the second axis of the analysis (Fig. 6A). The dotted arrows represent the difference between the ordination of the biological (origins of arrows) and physico-chemical parameters (arrowheads). The principal component analysis (PCA) of physico-chemical parameters shows that samples at the bottom of the column were associated with lower pH values and higher dissolved As concentrations, at the opposite to those at the middle and upper levels of the column (Fig. 6B). *Acidithiobacillus* were more abundant in the upper level of the column according the PCA of the dominant bacterial taxa (Fig. 6C).

Iron and S were positively correlated with *Thiomonas* and *Metallibacterium*, but negatively with *Desulfosporosinus* (Fig. 6B and 6C). A positive correlation was observed between pH and *Microbacter*, whereas pH correlated negatively with *Cellulomonas* and

Luteococcus. Cellulomonas and *Luteococcus* were also correlated positively with As, unlike *Microbacter*.

Discussion

Removal of As and Sb along the experiment

The upflow anaerobic fixed-bed bioreactor efficiently removed As, Sb and some metals (Pb, Tl and Zn) present in a real arsenic-rich AMD water amended with Sb. Antimony removal was efficient even when Sb concentration was increased: it averaged 97% for initial concentrations 0.7 mM (phase 2) and 1.01 mM (phase 3). The improvement of Sb sulfide precipitation by lowering pH was observed by Chen et al. (2020), however their experimental condition was less acidic (pH 6.5) than ours. Here, more than 96% of As was removed inside the column reactor even with the increase of Sb concentration in the feeding water. Similarly, Liu et al. (2018) reported the concomitant precipitation of As and Sb (up to 98.2% and 99.4%) from synthetic neutral pH solution containing 0.07 mM of As(V) and 0.04 mM Sb(V), by bacterial sulfate-reduction. Here, the increase in the fed Sb concentration did not affect As bio-precipitation. Increasing the total metalloids concentration in the feed might have allowed a more efficient and rapid consumption of dissolved sulfide, in particular near the acidic feed supply at the bottom of the reactor, thus decreasing the toxicity-related stress of bacteria induced by H_2S in acidic conditions.

The SEM-EDS observations strongly suggest that As and Sb precipitated inside the reactor as solid sulfides. Li et al. (2022) already observed by SEM-EDS precipitates of amorphous precipitates identified as Sb_2S_3 in their batch culture of SRB grown in presence of high Sb concentrations. These As and Sb sulfide phases were detected in zones showing rod bacterial shapes, possibly because they precipitated around the cell that excreted the dissolved sulfide.

Such a phenomenon was already observed in batch conditions with As sulfide precipitating as coatings around bacterial cells growing in batch (Le Pape et al., 2017) and continuous (Battaglia-brunet et al., 2021) conditions with AMD from Carnoulès site. Liu et al. (2018) suggested that As adsorption could occur on already formed sulfides. As a global way, the sorption/co-precipitation of As with metal sulfides was suggested by other studies (Jong and Parry, 2003; Sahinkaya et al., 2015). Among them, Fe sulfides were regularly cited to enhance the removal of As inside sulfate-reducing bioreactor (Luo et al., 2008; Altun et al., 2014; Liu et al., 2018). In our column, the soluble Fe and S concentrations varied in a similar way, suggesting their concomitant precipitation. However, the elemental map and the low Fe signals in EDS spectra indicated a minor presence of Fe sulfide in Sb-As-bearing phases. Then, Fe does not appear to play a significant role in the removal of As or Sb in the present study. This difference of behaviour with previous studies can be explained by the stronger acidic condition of our experiment that favoured the precipitation of As and Sb as sulfide minerals (Le Pape et al., 2017; Han et al., 2018).

Bacterial diversity and key functional groups

The bacterial communities colonising the bioreactor resulted from inoculation with a microbial consortium including sulfate-reducing bacteria, originating from the AMD of Carnoulès. Most of the taxa identified in the inoculum and in the bioreactor were previously observed in the Carnoulès ecosystem (Delavat et al., 2012 and 2013) and in anaerobic bioreactors treating artificial or real mine effluents by sulfate reduction (Battaglia-Brunet et al., 2012; Sánchez-Andrea et al., 2014). A single known SRB was detected inside the reactor, affiliated to the genus *Desulforosporinus*, which is in agreement with previous finding in similar systems (Battaglia-Brunet et al., 2012; 2021). This genus includes acid tolerant SRB isolated from mining environment (Kimura et al., 2006; Church et al., 2007; Alazard et al., 2010; Jameson et al., 2010; Sánchez-Andrea et al., 2015; Mardanov et al., 2016; Panova et al.,

2021). It was the main bacterium composing the sulfate-reducing microbial consortium inoculated in the bioreactor, and was maintained inside the column, being often one of the main (bottom and/or middle levels in phases 1 and 2) and even the dominant (bottom level in phase 3) genus. Its relative abundance represented thus a considerable portion of the microbial community inside the reactor (up to 76.5 ± 5.9% in liquid and 81.0 ± 1.3% in bioprecipitates). Bacterial communities gathering SRB, fermenters and cellulolytic bacteria have already been observed in bioreactors treating mine water (Morales et al., 2005; Pruden et al., 2007; Pereyra et al., 2008 and 2010; Vasquez et al., 2016). In the bioreactor, interactions between the different identified metabolic groups are expected. Fermentative bacteria able to degrade complex organic molecules accounted for a large proportion of the detected genera. Members of the *Cellulomonas* genus are able to degrade cellulose and other complex polysaccharides (Lynd et al., 2002) and were already found associated to acidophilic SRB consortia (Dev et al., 2021). Cellulose degraders (*Cellulomonas*) and fermenters (*Microbacter* and *Luteococcus*) may possibly be able to depolymerise and consume sugars from the agar phase, and generate metabolites for SRB. The genus *Microbacter* has been first discovered in an acid rock drainage of the Rio Tinto and is described as an anaerobic propionigenic bacterium able to produce propionate, lactate and acetate from various sugars (Sánchez-Andrea et al., 2014). *Luteococcus*, a genus belonging to the Propionibacteraceae family, which members are known to produce mainly acetate, propionate and CO_2 from sugar fermentation (Stackebrandt et al., 2006), is consistently detected inside the column, although at lower proportion. More precisely, the OTU sequence classified within the genus *Luteococcus* matches with that of the acidophilic Propionibacteraceae strain H7p isolated from sediment of the Carnoulès AMD (Delavat et al., 2012). SRB might use metabolites produced by the complex polysaccharides degraders and the fermenters as carbon and energy sources. Association of these diverse metabolic groups inside an anaerobic process can promote synergic activities (Logan et al.,

2005; Pereyra et al., 2010; Sánchez-Andrea et al., 2014; Vasquez et al., 2016). *Desulfosporosinus* species usually oxidise organic compounds incompletely, producing acetate (Alazard et al., 2010; Mayeux et al., 2013; Sánchez-Andrea et al., 2015; Vandieken et al., 2017); however, a recent study has reported complete oxidation of propionate, lactate, and acetate to CO_2 by a *Desulfosporosinus* strain (Hausmann et al., 2019). On another hand, as the bioreactor was fed with glycerol, a well-known substrate for acidotolerant *Desulfosporosinus* strains but also a substrate for *Cellulomonas* and Propionibacteraceae, a competition for glycerol may also occur and limit the organic carbon availability for SRB. As some anaerobic bacteria can perform fermentation of tartrate (Schink et al., 1984), the supply of this organic acid (with Sb) as additional potential electron donor, i.e. 0.7 mM in phase 2 and up to 1 mM during phase 3, could also contribute to influence the evolution of bacterial community composition during the experiment. *Acidocella* is a heterotrophic acidophilic genus that also presents a metabolic interest. For instance, *Acidocella aromatica* uses a limited range of organic substrates, such as acetate (Jones et al., 2013; Ňancucheo et al., 2016). Acetate is a toxic compound at low pH, potentially produced by several bacteria in our system, including SRB. In 2006, Kimura et al. proposed a syntrophic interaction between *Acidocella* and *Desulfosporosinus*. *Acidocella* generated carbon dioxide and hydrogen from the acetate produced by *Desulfosporosinus*, hydrogen being used as electron donor by *Desulfosporosinus*. In our system, *Acidocella* was mainly present in phases 1 and 2, and might have been replaced by other acetate degraders in phase 3.

Relation between the bacterial communities, the physico-chemical parameters, and the sulfate reducing activity

There was a clear evolution in both space and time of the taxonomic composition of bacterial communities inside the column (Fig. 6). The co-inertia analysis showed a significant correlation between the evolution of biological and some physico-chemical parameters. As a fact, pH, S, As and Sb concentrations were among the most important factors explaining the percentages of the main bacterial genera (Fig. 6). However, these parameters are directly influenced by the sulfate-reducing reaction which consumes H^+ and SO_4^{2-}, and leads to the precipitation of As and Sb as sulfides. Sulfate reduction occurred inside the column, as evidenced by the decrease of dissolved S concentration and metal sulfide precipitation, and the gradual increase of pH in the bioreactor. In the liquid samples, the higher proportion of *Desulfosporosinus*-related OTU at the bottom of the column during the phase 1 and 3 is in agreement with the increase of pH between the inlet and the bottom of the column, but also with the As and Sb precipitation between the bottom and the middle of the column. The lowest precipitation efficiency was observed during phase 2 (Fig. 3), corresponding to the lowest feed pH and lowest proportion of *Desulfosporosinus*-related OTU at the bioreactor bottom (Fig. 6). The highest proportion of this sulfate reducing bacterium was found in the bio-precipitates suggesting that *Desulfosporosinus* was mainly present in the biofilm compartment. This may be linked to the development of micro-environments that protected the cells against stressing parameters such as acidity or oxygen diffusion from the outlet (Yin et al., 2019; Tran et al., 2021). The presence of *Acidithiobacillus*- and *Thiomonas*-related OTU in the upper zone of the bioreactor, that appeared red coloured (SM4), may be linked to oxygen diffusion from the top of the column. *Acidithiobacillus* and *Thiomonas* are S- and Fe-oxidising bacteria already detected in Carnoulès site (Delavat et al., 2012, 2013). The glycerol fed at the bottom of the bioreactor could explain higher proportions of *Cellulomonas*, *Luteococcus* and *Desulfosporosinus* (all genera consuming this substrate) in the bottom zone of the bioreactor (Fig. 6). The metabolism of organic substrates might have exerted influence

on the dynamics of the bacterial community. Hessler et al. (2018) observed a stratification of microbial communities throughout a biological sulfate-reducing up-flow anaerobic packed bed reactor that was attributed to variations of lactate and the volatile fatty acids produced by microbial metabolisms. Further analyses would be required in order to determine the effect of organic molecules resulting from the metabolism of glycerol and tartrate and biodegradation of agar, on the diversity and structure of bacterial communities.

Globally, this study demonstrated for the first time the possibility to remove concomitantly As and Sb as sulfides in a continuous column bioreactor fed with a real AMD. The reactor removed up to 98%-99% of dissolved As and Sb, with no competition between As and Sb for precipitation with sulfides when they co-occurred at concentrations up to 1 mM each in the AMD. *Desulfosporosinus*, the only known SRB genus detected in the bioreactor, was present as a major contributor to the bacterial community, which also included polymers degraders and fermenters. The biological reduction of the sulfate contained in the AMD provided enough dissolved sulfide to precipitate efficiently As and Sb. The co-occurrence of SRB, polymers degraders and fermenters can be an advantage for future *in situ* passive treatment of AMD, in the perspective to use low-cost complex organic substrates to sustain long-term bacterial activity in a bioreactor. Results are promising for the perspective of passive bio-treatments of AMD containing metalloids.

Acknowledgements

This research was co-funded by ADEME, the French Agency for the Environment and Energy Management (convention TEZ16-22), and BRGM. Rémi Freydier and Léa Causse are acknowledged for ICP-MS analysis. The authors thank the MetaHealth metagenomic-based

services (CIRAD, PHIM, Eco&Sols, Montpellier, France) for MiSeq illumina sequencing. We thank Chris Bryan for english style verification.

References

Alam R, McPhedran K. Applications of biological sulfate reduction for remediation of arsenic – A review. *Chemosphere* 2019;**222**:932-944. https://doi.org/10.1016/j.chemosphere.2019.01.194

Alazard D, Joseph M, Battaglia-Brunet F et al. *Desulfosporosinus acidiphilus* sp. nov.: a moderately acidophilic sulfate-reducing bacterium isolated from acid mining drainage sediments : New taxa: *Firmicutes* (Class *Clostridia*, Order *Clostridiales*, Family *Peptococcaceae*). *Extremophiles* 2010;**14**:305-312. https://doi.org/10.1007/s00792-010-0309-4

Altun M, Sahinkaya E, Durukan I et al. Arsenic removal in a sulfidogenic fixed-bed column bioreactor. *J Haz Mat* 2014;**269**:31-37. https://doi.org/10.1016/j.jhazmat.2013.11.047

Afgan E, Baker D, Batut B et al. The Galaxy platform for accessible, reproducible and collaborative biomedical analyses: 2018 update. *Nucleic Acids Res* 2018;**46**:W537-W544. https://doi.org/10.1093/nar/gky379

Battaglia-Brunet F, Crouzet C, Burnol A et al. Precipitation of arsenic sulphide from acidic water in a fixed-film bioreactor. *Wat Res* 2012;**46**:3923-3933. https://doi.org/10.1016/j.watres.2012.04.035

Battaglia-Brunet F, Casiot C, Fernandez-Rojo L et al. Laboratory-Scale Bio-Treatment of Real Arsenic-Rich Acid Mine Drainage. *Wat Air and Soil Poll* 2021:**232**:330. https://doi.org/10.1007/s11270-021-05276-z

Bokulich NA, Subramanian S, Faith JJ et al. Quality-filtering vastly improves diversity estimates from Illumina amplicon sequencing. *Nat Methods* 2013;**10**:57-59. https://doi.org/10.1038/nmeth.2276

Cidu R, Biddau R, Dore E et al. Antimony in the soil-water-plant system at the Su Suergiu abandoned mine (Sardinia, Italy): strategies to mitigate contamination. *Sci Total Environ* 2014 ;**497–498** :319-331. https://doi.org/10.1016/j.scitotenv.2014.07.117

Chemidlin Prévost-Bouré N, Christen R, Dequiedt S et al. Validation and application of a PCR primer set to quantify fungal communities in the soil environment by real-time quantitative PCR. *PLoS One* 2011;6(9):e24166. doi:10.1371/journal.pone.0024166

Chen J, Zhang G, Ma C et al. Antimony removal from wastewater by sulfate-reducing bacteria in a bench-scale upflow anaerobic packed-bed reactor. *Acta Geochim* 2020; **39**:203-215. https://doi.org/10.1007/s11631-019-00382-6

Church CD, Wilkin RT, Alpers CN, Rye RO et al. Microbial sulfate reduction and metal attenuation in pH 4 acid mine water. *Geochem Trans* 2007;**8**:10. https://doi.org/.1186/1467-4866-8-10

Core Team. R: A language and environment for statistical computing. R Foundation for Statistical Computing. 2018. Vienna, Austria. https://www.R-project.org

Council of the European Communities (76/464/EEC) of 4 May 1976 on pollution caused by certain dangerous substances discharged into the aquatic environment of the Community. Official Journal L 129, 0023–0029. European Environment Agency. www.eea.europa.eu/policy-documents/council-directive-76-464-eec (accessed 2.5.19)

Cullen WR, Reimer KJ. Arsenic speciation in the environment. *Chem Rev* 1989;**89**:713-764. https://doi.org/10.1021/cr00094a002

Delavat F, Lett MC, Lièvremont D. Novel and unexpected bacterial diversity in an arsenic-rich ecosystem revealed by culture-dependent approaches. *Biol Direct* 2012;**7**:28. https://doi.org/10.1186/1745-6150-7-28

Delavat F, Lett MC, Lièvremont D. Yeast and bacterial diversity along a transect in an acidic, As-Fe rich environment revealed by cultural approaches. *Sci Total Environ* 2013;**463-464**: 823-828. https://doi.org/10.1016/j.scitotenv.2013.06.023

Dev S, Galey M, Chun CL et al. Enrichment of psychrophilic and acidophilic sulfate-reducing bacterial consortia – a solution toward acid mine drainage treatment in cold regions. *Environ Sci: Processes Impacts* 2021;**23**:2007-2020. https://doi.org/10.1039/D1EM0025

Dray S, Dufour AB. The ade4 Package: implementing the duality diagram for ecologists. *J Stat Softw* 2007;**22**:1-20. https://doi.org/10.18637/jss.v022.i04

Edgar RC, Haas BJ, Clemente JC et al. UCHIME improves sensitivity and speed of chimera detection. *Bioinformatics* 2011;**27**:2194-2200. https://doi.org/10.1093/bioinformatics/btr381

Escudié F, Auer L, Bernard M et al. FROGS: Find, Rapidly, OTUs with Galaxy Solution. *Bioinformatics* 2018 ;**34**:1287-1294. https://doi.org/10.1093/bioinformatics/btx791

Filella M, Belzile N, ChenYW. Antimony in the environment: a review focused on natural waters: I. Occurrence. Earth-Sci Rev 2002;**57**:125–176. https://doi.org/10.1016/S0012-8252(01)00070-8

Han YS, Seong HJ, Chon CM et al. Interaction of Sb(III) with iron sulfide under anoxic conditions: Similarities and differences compared to As(III) interactions. *Chemosphere* 2018; 195 :762-770. https://doi.org/10.1016/j.chemosphere.2017.12.133

Hausmann B, Pelikan C, Rattei T et al. Long-Term Transcriptional Activity at Zero Growth of a Cosmopolitan Rare Biosphere Member. *mBio* 2019;**10**:e02189-18. https://doi.org/10.1128/mBio.02189-18

He M, Wang N, Long X et al. Antimony speciation in the environment: Recent advances in understanding the biogeochemical processes and ecological effects. *J Environ Sci* 2019;**75**: 14-39. https://doi.org/10.1016/j.jes.2018.05.023

Herath I, Vithanage M, Bundschuh J. Antimony as a global dilemma: Geochemistry, mobility, fate and transport. *Environ Pollut* 2017;**223**:545-559. https://doi.org/10.1016/j.envpol.2017.01.057

Hessler T, Harrison STL, Huddy RJ. Stratification o*f microbial communities throughout a biological sulphate reducing up-flow anaerobic packed bed reactor, revealed through 16S metagenomics. *Res Microbiol* 2018 ;**169**:543-551. https://doi.org/10.1016/j.resmic.2018.09.003

Inam MA, Khan R, Park DR et al. Influence of pH and Contaminant Redox Form on the Competitive Removal of Arsenic and Antimony from Aqueous Media by Coagulation. *Minerals* 2018;**8**:574. https://doi.org/10.3390/min8120574

Jameson E, Rowe OF, Hallberg KB et al. Sulfidogenesis and selective precipitation of metals at low pH mediated by *Acidithiobacillus* spp. and acidophilic sulfate-reducing bacteria. *Hydrometallurgy* 2010;**104**:488–493. https://doi.org/10.1016/j.hydromet.2010.03.029

Jones RM, Hedrich S, Johnson DB. *Acidocella aromatica* sp. nov.: an acidophilic heterotrophic alphaproteobacterium with unusual phenotypic traits. *Extremophiles* 2013;**17**:841-850. https://doi.org/10.1007/s00792-013-0566-0

Jong T, Parry DL. Removal of sulfate and heavy metals by sulfate reducing bacteria in short-term bench scale upflow anaerobic packed bed reactor runs. *Wat Res* 2003;**37**:3379-3389. https://doi.org/10.1016/S0043-1354(03)00165-9

Kimura S, Hallberg KB, Johnson DB. Sulfidogenesis in low pH (3.8-4.2) media by a mixed population of acidophilic bacteria. *Biodegradation* 2006;**17**:159-167. https://doi.org/10.1007/s10532-005-3050-4

Kujala K , Laamanen T, Khan UA et al. Kinetics of arsenic and antimony reduction and oxidation in peatlands treating mining-affected waters: Effects of microbes, temperature, and carbon substrate. Soil Biol Biochem 2022; 108598. https://doi.org/10.1016/j.soilbio.2022.108598

Lan B, Wang Y, Wang X et al. Aqueous arsenic (As) and antimony (Sb) removal by potassium ferrate. *Chem Eng J* 2016;**292**:389-397. https://doi.org/10.1016/j.cej.2016.02.019

Laroche E, Casiot C, Fernandez-Rojo L et al. Dynamics of Bacterial Communities Mediating the Treatment of an As-Rich Acid Mine Drainage in a Field Pilot. *Front Microbiol* 2018 ;**9**, 3169. https://doi.org/10.3389/fmicb.2018.03169

Legendre P, Gallagher ED. Ecologically meaningful transformations for ordination of species data. *Oecologia* 2001;**129**:271-280. https://doi.org/10.1007/s004420100716

Le Pape P, Battaglia-Brunet F, Parmentier M et al. Complete removal of arsenic and zinc from a heavily contaminated Acid Mine Drainage via an indigenous SRB consortium. *J Haz Mat* 2017;**321**:764-772. https://doi.org/10.1016/j.jhazmat.2016.09.060

Li H, Fei Y, Xue S et al. Removal of Antimony in Wastewater by Antimony Tolerant Sulfate-Reducing Bacteria Isolated from Municipal Sludge. *Int J Mol Sci* 2022;**23**:1594. https://doi.org/10.3390/ijms23031594

Liu F, Zhang G, Liu S et al. Bioremoval of arsenic and antimony from wastewater by a mixed culture of sulfate-reducing bacteria using lactate and ethanol as carbon sources. *Int Biodet Biodegradation* 2018;**126**:152-159. https://doi.org/10.1016/j.ibiod.2017.10.011

Logan MV, Reardon KF, Figueroa LA et al. Microbial community activities during establishment, performance, and decline of bench-scale passive treatment systems for mine drainage. *Wat Res* 2005;39:4537-4551. https://doi.org/10.1016/j.watres.2005.08.013

Luo Q, Tsukamoto TK, Zamzow KL et al. Arsenic, Selenium, and Sulfate Removal using an Ethanol-Enhanced Sulfate-Reducing Bioreactor. *Mine Water Environ* 2008;**27**:100-108. https://doi.org/10.1007/s10230-008-0032-x

Lynd LR, Weimer PJ, Zyl WH et al. Microbial Cellulose Utilization: Fundamentals and Biotechnology. *Microbiol Mol Biol Rev* 2002;66:506-577. https://doi.org/10.1128/MMBR.66.3.506-577.2002

Mahé F, Rognes T, Quince C et al. Swarm: robust and fast clustering method for amplicon-based studies. *Peer J* 2014;**2**:e593. https://doi.org/10.7717/peerj.593

Manaka M, Yanase N, Sato T et al. Natural attenuation of antimony in mine drainage water. *Geochem J* 2007 ;**41**:17–27. https://doi.org/10.2343/geochemj.41.17

Mardanov AV, Panova IA, Beletsky AV et al. Genomic insights into a new acidophilic, copper-resistant *Desulfosporosinus* isolate from the oxidized tailings area of an abandoned gold mine. *FEMS Microbiol Ecol* 2016;**92**:fiw111. https://doi.org/10.1093/femsec/fiw111

Mayeux B, Fardeau ML, Bartoli-Joseph M et al. *Desulfosporosinus burensis* sp. nov., a spore-forming, mesophilic, sulfate-reducing bacterium isolated from a deep clay environment. Int J Syst Evol Microbiol 2013;**63**:593–598. https://doi.org/10.1099/ijs.0.035238-0

Michel C, Baran N, André L et al. Side effects of pesticides in groundwater: impact on bacterial denitrification *Front Microbiol* 2021;**12**:662727. https://doi.org//10.3389/fmicb.2021.662727

Morales TA, Dopson M, Athar R et al. Analysis of bacterial diversity in acidic pond water and compost after treatment of artificial acid mine drainage for metal removal. *Biotechnol Bioeng* 2005;**90**:543-551. https://doi.org/10.1002/bit.20421

Ňancucheo I, Johnson DB. Selective removal of transition metals from acidic mine waters by novel consortia of acidophilic sulfidogenic bacteria. Microbial Biotechnol. 2012;**5**:34-44. https://doi.org/10.1111/j.1751-7915.2011.00285.x

Ňancucheo I, Johnson DB. Removal of sulfate from extremely acidic mine waters using low pH sulfidogenic bioreactors. *Hydrometallurgy* 2014;**150**:222-226. https://doi.org/10.1016/j.hydromet.2014.04.025

Ňancucheo I, Rowe OF, Hedrich S et al. Solid and liquid media for isolating and cultivating acidophilic and acid-tolerant sulfate-reducing bacteria. *FEMS Microbiol Lett* 2016;**363**: fnw083. https://doi.org/10.1093/femsle/fnw083

Paikaray S. Arsenic Geochemistry of Acid Mine Drainage. *Mine Wat Environ* 2015 ;**34** :181-196. https://doi.org/1007/s10230-014-0286-4

Panova IA, Ikkert O, Avakyan MR et al. *Desulfosporosinus metallidurans* sp. nov., an acidophilic, metal-resistant sulfate-reducing bacterium from acid mine drainage. *Int J Syst Evol Microbiol* 2021;**71**:7. https://doi.org/10.1099/ijsem.0.004876

Pereyra LP, Hiibel SR, Pruden A et al. Comparison of microbial community composition and activity in sulfate-reducing batch systems remediating mine drainage. *Biotechnol Bioeng* 2008;**101**:702-713. https://doi.org/10.1002/bit.21930

Pereyra LP, Hiibel SR, Riquelme MVP et al. Detection and Quantification of Functional Genes of Cellulose- Degrading, Fermentative, and Sulfate-Reducing Bacteria and Methanogenic Archaea. *Appl Environ Microbiol* 2010;**76**:2192-2202. https://doi.org/10.1128/AEM.01285-09

Planer-Friedrich B, Scheinost AC. Formation and Structural Characterization of Thioantimony Species and Their Natural Occurrence in Geothermal Waters. *Environ Sci Technol* 2011;**45**:6855-6863. https://doi.org/10.1021/es201003k

Pruden A, Messner N, Pereyra L et al. The effect of inoculum on the performance of sulfate-reducing columns treating heavy metal contaminated water. *Wat Res* 2007;**41**:904-914. https://doi.org/10.1016/j.watres.2006.11.025

Qi P, Pichler T. Competitive adsorption of As(III), As(V), Sb(III) and Sb(V) onto ferrihydrite in multi-component systems: Implications for mobility and distribution. *J Haz Mat* 2017;**330**:142-148. https://doi.org/10.1016/j.jhazmat.2017.02.016

Resongles E, Casiot C, Elbaz-Poulichet F et al. Fate of Sb(V) and Sb(III) species along a gradient of pH and oxygen concentration in the Carnoulès mine waters (Southern France). *Environ Sci: Processes Impacts* 2013 ;15 :1536-1544. https://doi.org/doi:10.1039/c3em00215b

Rognes T, Flouri T, Nichols B et al. VSEARCH: a versatile open source tool for metagenomics. *Peer J* 2016;**4**:e2584. https://doi.org/10.7717/peerj.2584

Sahinkaya E, Yurtsever A, Toker Y et al. Biotreatment of As-containing simulated acid mine drainage using laboratory scale sulfate reducing upflow anaerobic sludge blanket reactor. Minerals Engineering, *Min Eng* 2015;**75**,133-139. https://doi.org/10.1016/j.mineng.2014.08.012

Sánchez-Andrea I, Sanz JL, Bijmans MFM et al. Sulfate reduction at low pH to remediate acid mine drainage. *J Haz Mat* 2014;269:98-109. https://doi.org/10.1016/j.jhazmat.2013.12.032

Sánchez-Andrea I, Stams AJM, Hedrich S et al. *Desulfosporosinus acididurans* sp. nov.: an acidophilic sulfate-reducing bacterium isolated from acidic sediments. *Extremophiles* 2015; 19:39-47. https://doi.org/10.1007/s00792-014-0701-6

Schink B. Fermentation of tartrate enantiomers by anaerobic bacteria, and description of two new species of strict anaerobes, *Ruminococcus pasteurii* and *Ilyobacter tartaricus*. *Arch Microbiol* 1984;**139**:409-414. https://doi.org/10.1007/BF00408388

Smedley PL, Kinniburgh DG. A review of the source, behaviour and distribution of arsenic in natural waters. *Appl Geochem* 2002;**17**:517-568. https://doi.org/10.1016/S0883-2927(02)00018-5

Skousen JG, Sexstone A, Ziemkiewicz PF. Acid Mine Drainage Control and Treatment. *Reclamation of Drastically Disturbed Lands* 2000.**41**:131-168. https://doi.org/10.2134/agronmonogr41.c6

Stackebrandt E, Cummins CS, Johnson JL. Family *Propionibacteriaceae*: The Genus *Propionibacterium*. In: Dworkin M, Falkow S, Rosenberg E, Schleifer K-H, Stackebrandt E (eds.). *The Prokaryotes Archaea. Bacteria: Firmicutes, Actinomycetes*. New York: Springer Science, 2006;**3**: 400-418. https://doi.org/10.1007/0-387-30743-5_19

Sun W, Xiao E, Kalin M et al. Remediation of antimony-rich mine waters: Assessment of antimony removal and shifts in the microbial community of an onsite field-scale bioreactor. *Environ Pollut* 2016;**215**:213-222. https://doi.org/10.1016/j.envpol.2016.05.008

Tran TTT, Kannoorpatti K, Padovan A et al. Sulphate-Reducing Bacteria's Response to Extreme pH Environments and the Effect of Their Activities on Microbial Corrosion. Appl Sci 2021;**11**:2201. https://doi.org/10.3390/app11052201

US EPA.Office of the Federal Registration (OFR) Appendix A: priority pollutants Fed Reg 47.

1982.

Vandieken V, Niemann H, Engelen B et al. *Marinisporobacter balticus* gen. nov., sp. nov., *Desulfosporosinus nitroreducens* sp. nov. and *Desulfosporosinus fructosivorans* sp. nov., new spore-forming bacteria isolated from subsurface sediments of the Baltic Sea. *Int J Syst Evol Microbiol* 2017;**67**:1887-1893. https://doi.org/10.1099/ijsem.0.001883

Vasquez YF, Escobar MCM, Neculita CM et al. Biochemical passive reactors for treatment of acid mine drainage: Effect of hydraulic retention time on changes in efficiency, composition of reactive mixture, and microbial activity. *Chemosphere* 2016;**153**,244-253. https://doi.org/10.1016/j.chemosphere.2016.03.052

Wang H, Chen F, Mu S et al. Removal of antimony (Sb(V)) from Sb mine drainage: Biological sulfate reduction and sulfide oxidation–precipitation. *Biores Technol* 2013;**146**-799802. https://doi.org/10.1016/j.biortech.2013.08.002

Wen Y, Wang Y, Liu L et al. Biofilms: The Microbial "Protective Clothing" in Extreme Environments. *Int J Mol Sci* 2019;**20**:3423. https://doi.org/10.3390/ijms20143423

Wu F, Fu Z, Liu B et al. Health risk associated with dietary co-exposure to high levels of antimony and arsenic in the world's largest antimony mine area. *Sci Total Environ* 2011;409: 3344-3351. https://doi.org/10.1016/j.scitotenv.2011.05.033

Wu D, Sun SP, He M et al. As(V) and Sb(V) co-adsorption onto ferrihydrite: synergistic effect of Sb(V) on As(V) under competitive conditions. *Environ Sci Pollut Res* 2018;**25**:14585-14594. https://doi.org/10.1007/s11356-018-1488-2

Xi Y, Lan S, Li X et al. Bioremediation of antimony from wastewater by sulfate-reducing bacteria: Effect of the coexisting ferrous ion. *Int Biodeter Biodegr* 2020;**148**:104912. https://doi.org/10.1016/j.ibiod.2020.104912

Zhang G, Ouyang X, Li H et al. Bioremoval of antimony from contaminated waters by a mixed batch culture of sulfate-reducing bacteria. *Int Biodeter Biodegr* 2016;**115**:148-155. https://doi.org/10.1016/j.ibiod.2016.08.007

Figure 1: Schematic representation of the upflow anaerobic fixed-bed bioreactor (A). Picture of the column with filling material and yellow biogenic precipitates (B).

Figure 2: pH variations of inlet and outlet waters represented by white and black circles respectively (A). Histogram of pH vertical-profiles at the end of each phase in the column bioreactor (B); the white circles represent the average pH of inlet and outlet waters along each phase, and the error bars indicate standard deviations of the mean for three measurements for each feed condition.

Figure 3: Vertical punctual profiles of dissolved arsenic (A), antimony (B, focus on low concentration C), iron (D) and sulphur (E) concentrations in the column bioreactor at the end of each phase (data missing for the Sb concentration in the inlet water in phase 1). Error bars indicate analytical error (2%). The white circles represent the average concentrations of inlet and outlet waters for each phase (three measures), and the error bars indicate standard deviations of the mean for three measurements for each feed condition.

Figure 4: SEM observation of bottom bioreactor filling at the end of experiment in backscattering electron mode showing biofilm morphology in a first zone (A) and the corresponding EDS spectrum (B), and another zone showing Sb-enriched aggregate (C) and the corresponding EDS spectrum (D).

Figure 5: Taxonomic composition of bacterial communities (at the genus level) in the inoculum, the liquid and the solid samples collected along the reactor at the end of each phases (analyses performed in triplicates except for the inoculum). "Others" represent the phylogenetic groups with a relative abundance < 1% calculated on the whole dataset.

Figure 6: Co-inertia analysis of the physico-chemical parameters and the dominant bacterial taxa at each position in the column. (A) Plot represents the projection of the samples, grouped according their position inside the column, on the first two co-inertia axes. The dotted arrows represent the difference between the ordination of the biological (origins of arrows) and physico-chemical parameters (arrowheads); dotted arrows length are inversely proportional to the strength of the relationship between parameters. The upper-left barplot indicates the eigenvalues. (B) PCA of the physico-chemical parameters at each position in the column. Chemical parameters are represented by their chemical symbols as: Fe (dissolved iron concentration), S (dissolved sulfur concentration), As (dissolved arsenic concentration) and Sb (dissolved antimony concentration). (C) PCA of the dominant bacterial taxa at each position in the column.

Figure 1

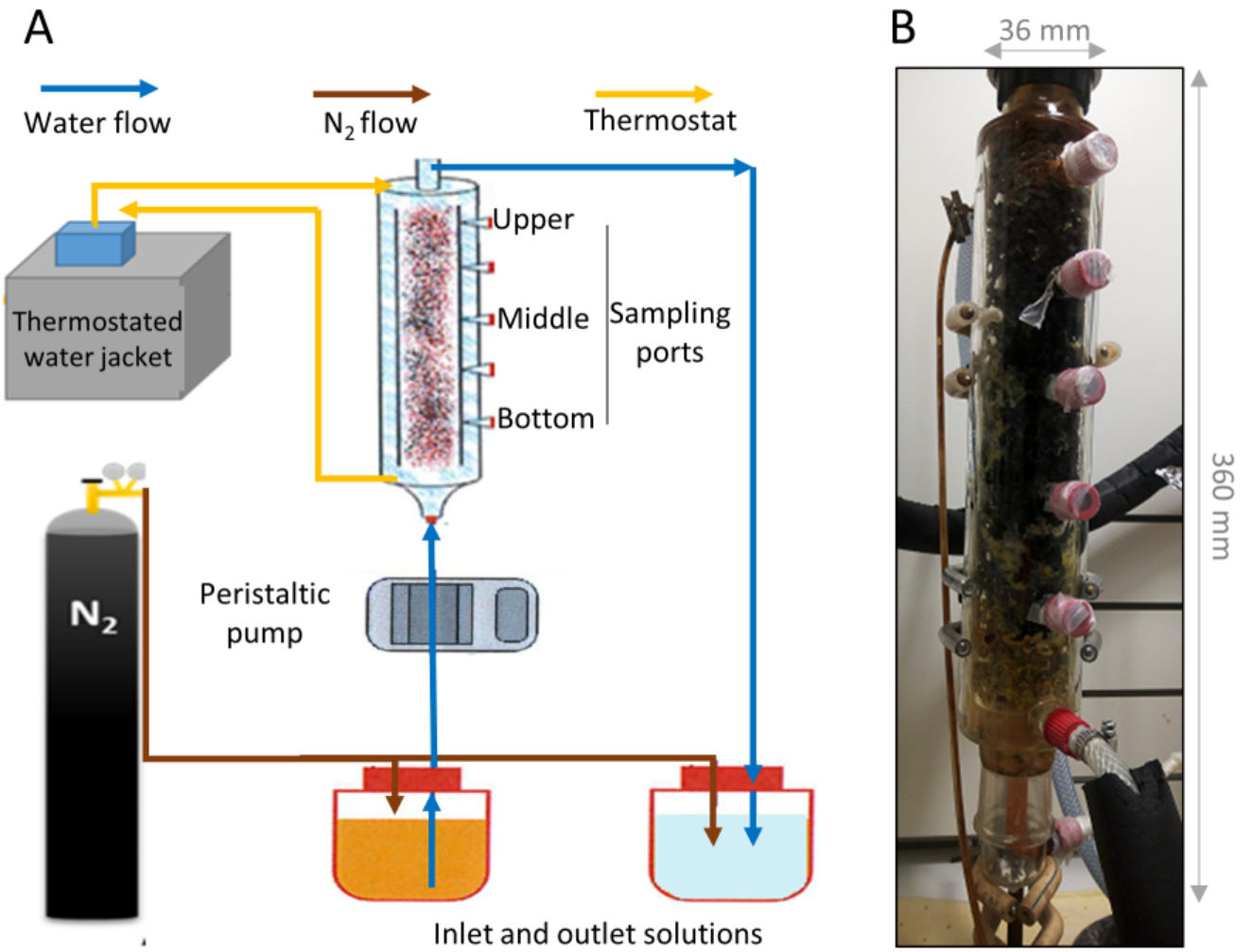
A
Water flow
N_2 flow
Thermostat
Thermostated water jacket
Upper
Middle
Bottom
Sampling ports
N_2
Peristaltic pump
Inlet and outlet solutions
B
36 mm
360 mm

Figure 2

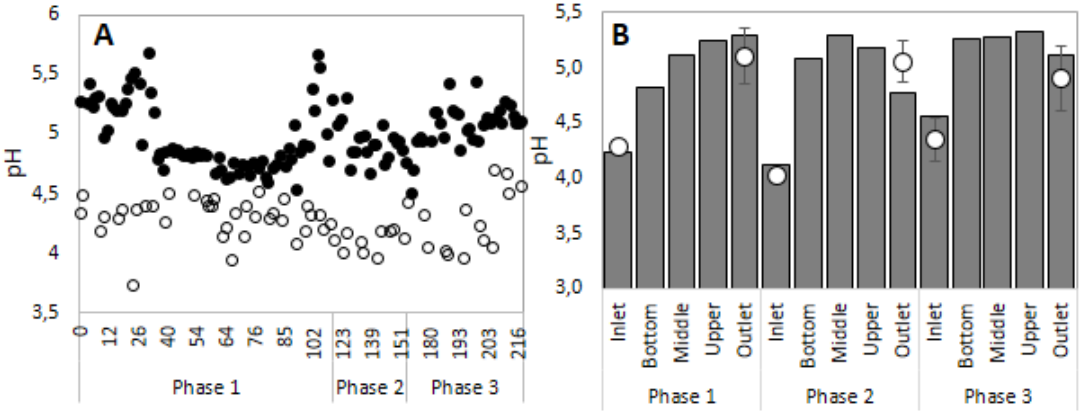
A
pH
6
5,5
5
4,5
4
3,5
0
12
26
40
54
64
76
85
102
123
139
151
180
193
203
216
Phase 1
Phase 2
Phase 3
B
pH
5,5
5,0
4,5
4,0
3,5
3,0
Inlet
Bottom
Middle
Upper
Outlet
Phase 1
Phase 2
Phase 3

Figure 3

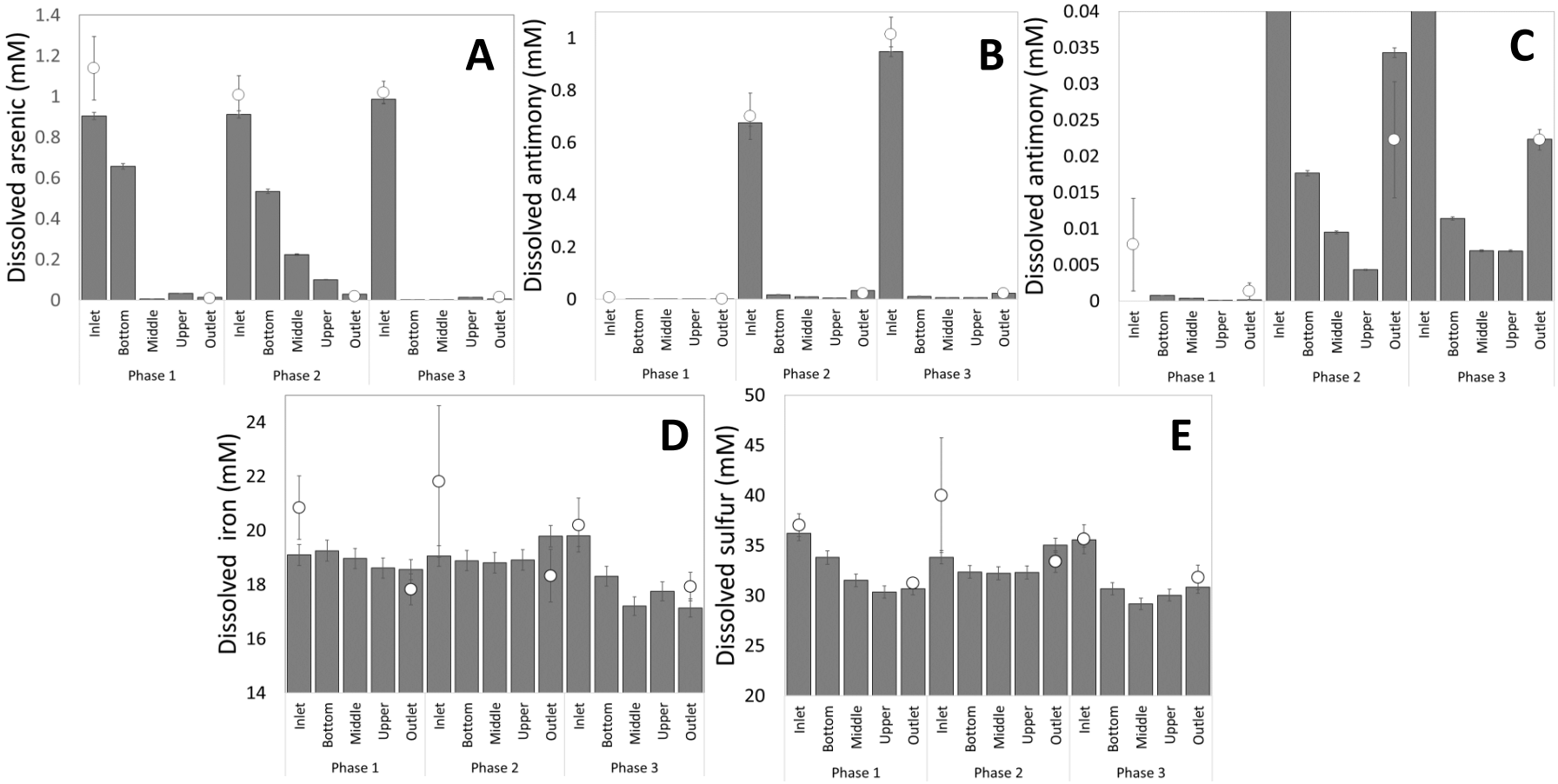
A
Dissolved arsenic (mM)
1.4
1.2
1
0.8
0.6
0.4
0.2
0
B
Dissolved antimony (mM)
1
0.8
0.6
0.4
0.2
0
C
Dissolved antimony (mM)
0.04
0.035
0.03
0.025
0.02
0.015
0.01
0.005
0
D
Dissolved iron (mM)
24
22
20
18
16
14
E
Dissolved sulfur (mM)
50
45
40
35
30
25
20
Inlet
Bottom
Middle
Upper
Outlet
Phase 1
Phase 2
Phase 3

Figure 4

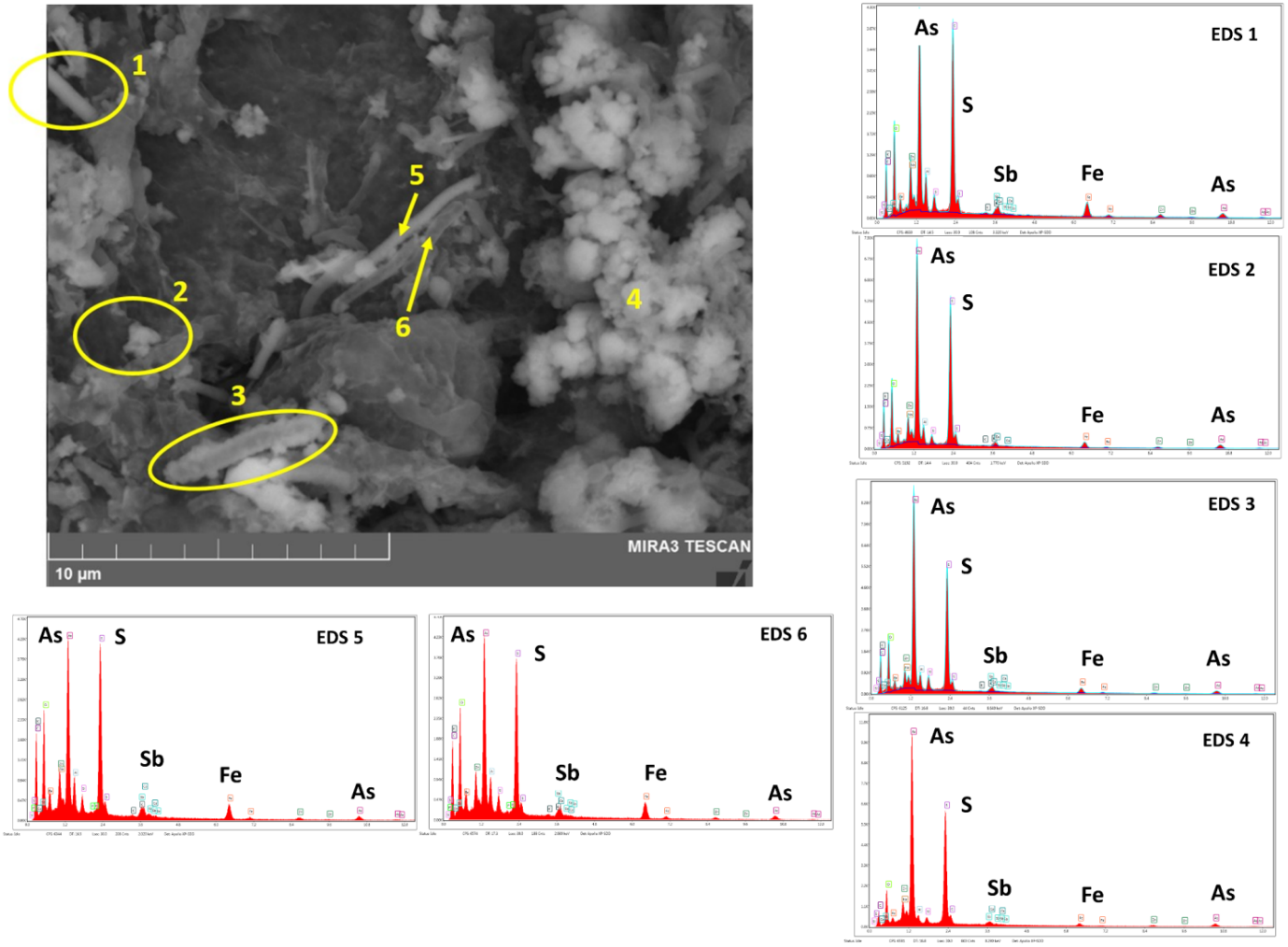
1
2
3
4
5
6
MIRA3 TESCAN
10 µm
EDS 1
EDS 2
EDS 3
EDS 4
EDS 5
EDS 6
As
S
Sb
Fe
As

Figure 5

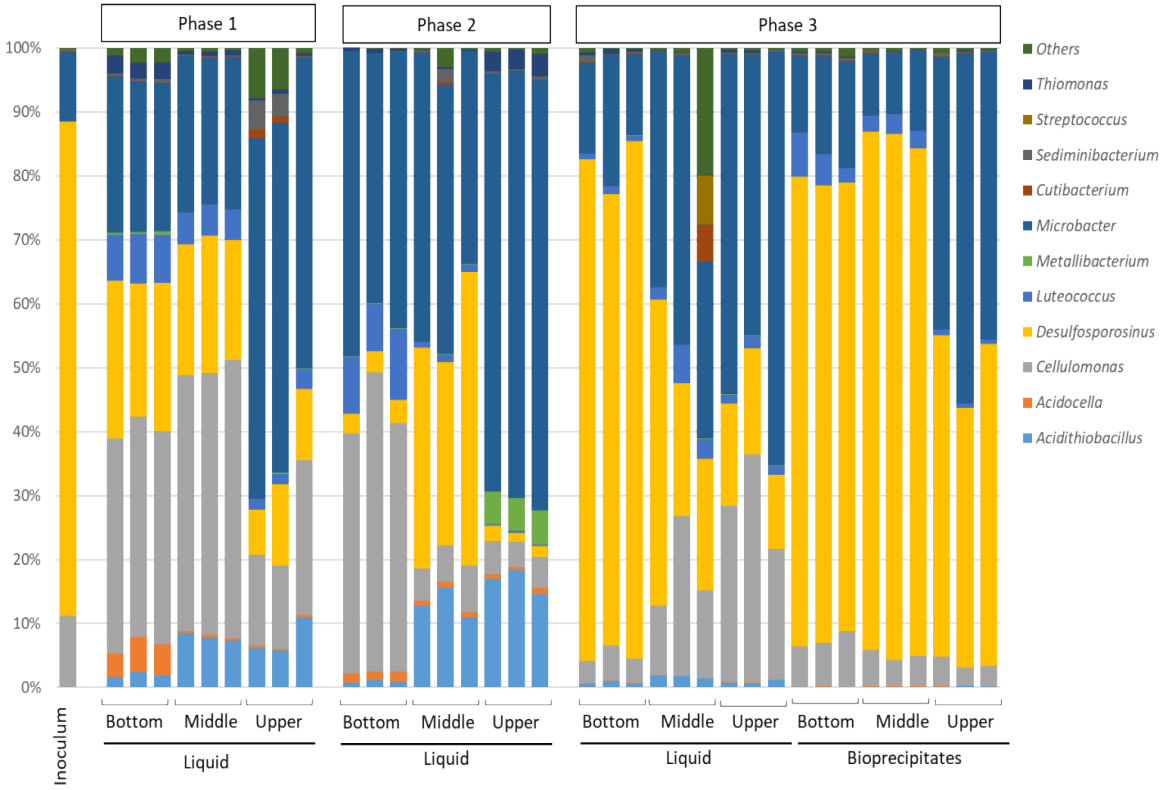
Phase 1
Phase 2
Phase 3
100%
90%
80%
70%
60%
50%
40%
30%
20%
10%
0%
Others
Thiomonas
Streptococcus
Sediminibacterium
Cutibacterium
Microbacter
Metallibacterium
Luteococcus
Desulfosporosinus
Cellulomonas
Acidocella
Acidithiobacillus
Inoculum
Bottom
Middle
Upper
Liquid
Bioprecipitates

Figure 6

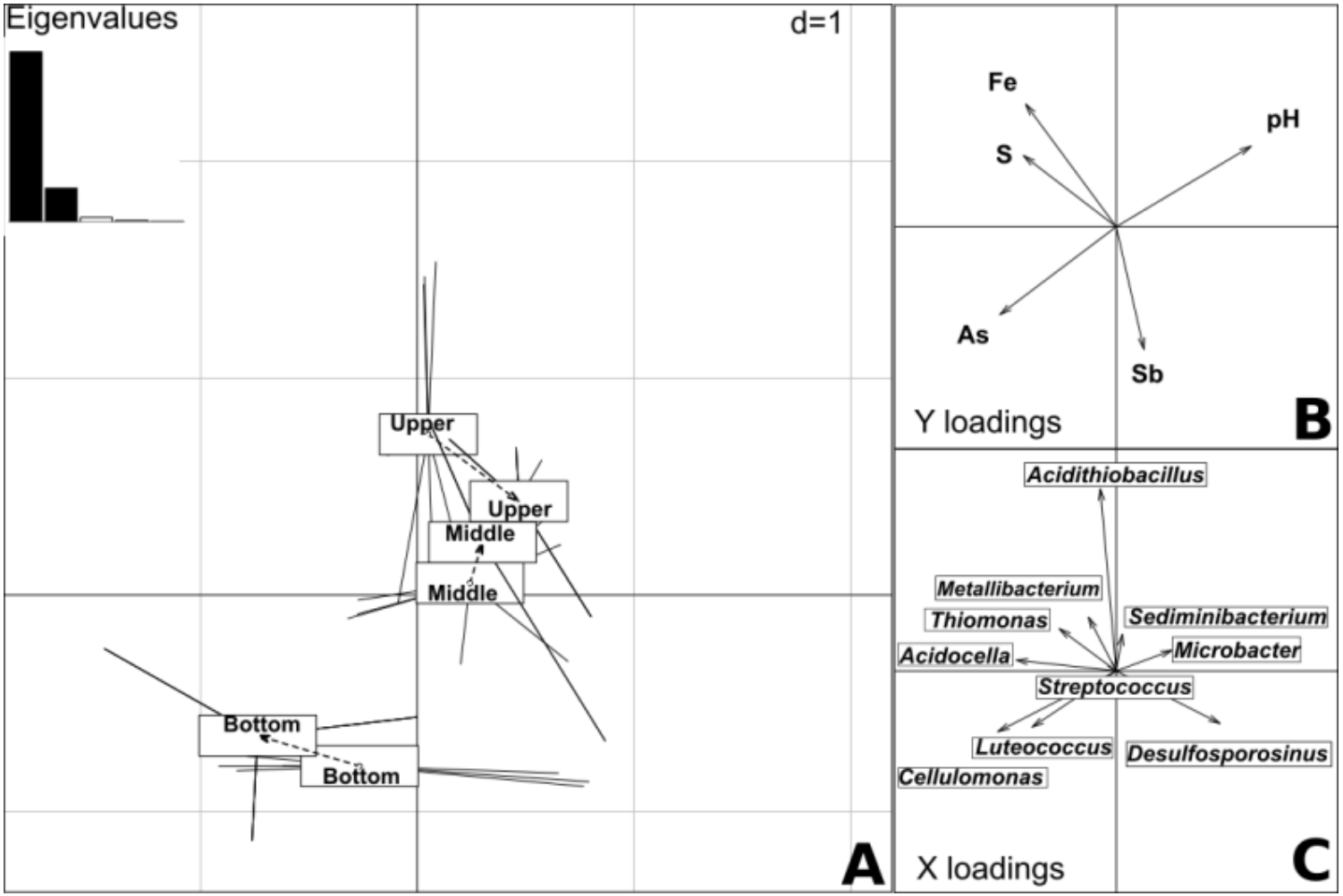
Eigenvalues
d=1
Upper
Upper
Middle
Middle
Bottom
Bottom
A
Fe
pH
S
As
Sb
Y loadings
B
Acidithiobacillus
Metallibacterium
Thiomonas
Sediminibacterium
Acidocella
Microbacter
Streptococcus
Luteococcus
Desulfosporosinus
Cellulomonas
X loadings
C

Table 1: Experimental conditions

Phase	Duration of the phase (days)	Sampling day for ICP-MS analysis	Flow (ml/h)*	Hydraulic retention Time (h)*	Feed pH*	Feed [As] (mM)*	Feed [Sb] (mM)*
1	117	0, 82 and 117	1.5 ± 0.1	132 ± 10	4.29 ± 0.03	1.14 ± 0.16	0.008 ± 0.006
2	35	123, 141 and 152	1.3 ± 0.1	163 ± 19	4.03 ± 0.06	1.01 ± 0.09	0.70 ± 0.09
3	65	152, 155, 204 and 217	1.4 ± 0.1	149 ± 15	4.35 ± 0.20	1.02 ± 0.06	1.01 ± 0.07

(*) average values

SM1. Average removal and concentrations of minor toxic elements from inlet and outlet waters during each phase.

	Phase		1	2	3
Pb	Concentration (mM)	Inlet	1.0 ± 0.9	0.7 ± 0.4	1.2 ± 0.5
		Outlet	$2 .10^{-3} \pm 2 .10^{-3}$	$< 2 .10^{-5}$	$4 .10^{-3} \pm 5 .10^{-3}$
	Removal (%)		99.9 ± 0.1	100	99.7 ± 0.4
Tl	Concentration (mM)	Inlet	$1.5 .10^{-3} \pm 1.0 .10^{-3}$	$1.5 .10^{-3} \pm 3.2 .10^{-2}$	$1.5 .10^{-3} \pm 6.2 .10^{-5}$
		Outlet	$2.1 .10^{-5} \pm 1.3 .10^{-5}$	$1.6 .10^{-5} \pm 1.1 .10^{-5}$	$2.0. 10^{-5} \pm 1.5 .10^{-6}$
	Removal (%)		98.7 ± 0.8	99.0 ± 0.8	98.7 ± 0.1
Zn	Concentration (mM)	Inlet	0.36 ± 0.02	0.38 ± 0.05	0.35 ± 0.05
		Outlet	$2.9. 10^{-3} \pm 1.9 .10^{-3}$	$9.8 .10^{-3} \pm 5.6 .10^{-3}$	$7.2 .10^{-3} \pm 9.0 .10^{-3}$
	Removal (%)		99.2 ± 0.5	97.4 ± 1.4	97.9 ± 2.7

SM2. SEM-EDS map showing the distribution of selected elements on bioprecipitate collected at the end of the experiment (middle zone of the column bioreactor).

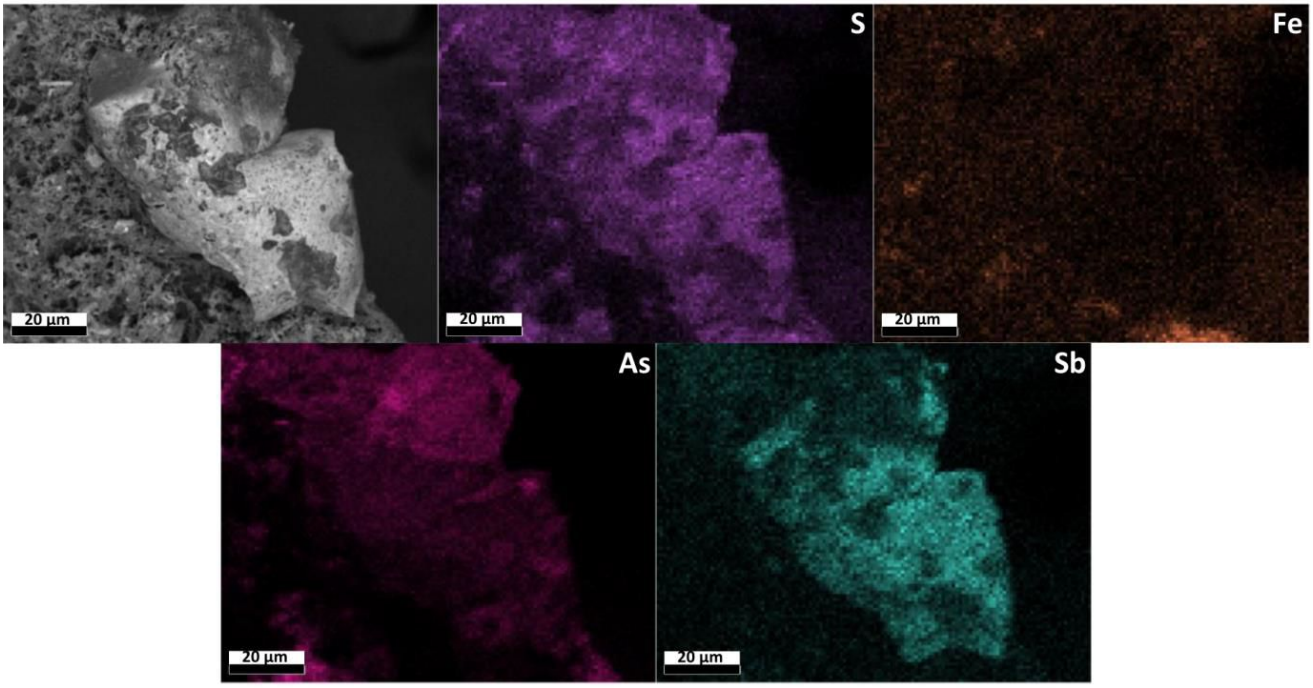

SM3.Bacterial Diversity indexes

Bacterial species richness in number of OTUs observed (A) and Shannon diversity index (B) in the liquid samples (solid lines) and solid samples (dashed lines) collected inside the reactor. The different letters represent significant differences between samples ($p < 0.05$).

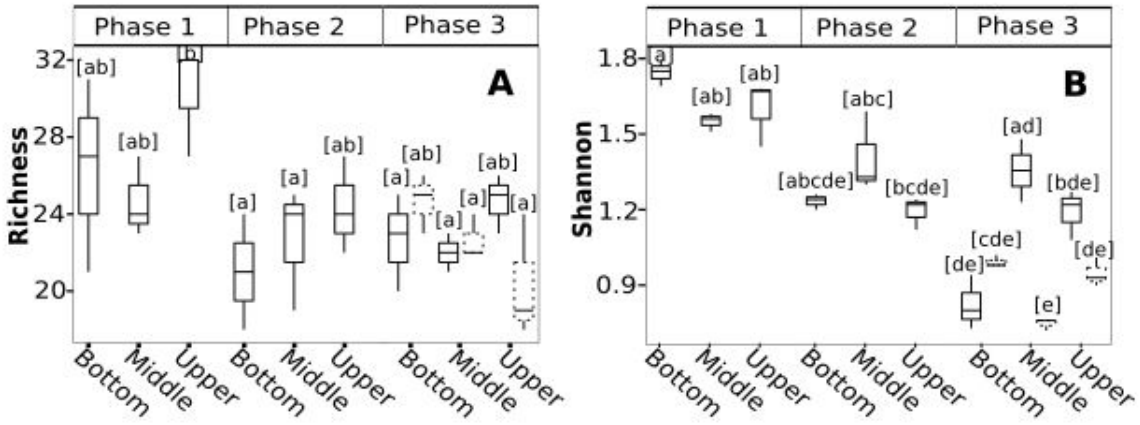

SM4. Pictures of the column bioreactor at the end of experiment

Bottom of the column bioreactor
At the end of experiment

Top of the column bioreactor
At the end of experiment